Spreading Factor Allocation for Massive Connectivity in LoRa Systems

Jin-Taek Lim and Youngnam Han

***Abstract*— Along with enhanced mobile broadband and ultra-reliable low latency communication, massive connectivity has been one of the key requirements for enabling technologies of 5G. For IoT, low power consumption and wide area coverage for end devices (ED) are important figures of merit, for which LoRa, SigFox and Narrow Band-IoT are dominant technologies. In this letter, we analyze LoRa systems for increasing average system packet success probability (PSP) under unslotted ALOHA random access protocol. The lower bound for average system PSP is derived by stochastic geometry. And it is shown that the average system PSP can be maximized by properly allocating spreading factor (SF) to each traffic, which also maximizes connectivity of EDs. We formulate an optimization problem for maximizing the average system PSP to propose a sub-optimal SF allocation scheme to each traffic. Analysis on PSP is validated through simulations, and comparison with existing schemes reveals that our proposed scheme achieves the highest PSP and so the maximum connectivity.**

***Index Terms*— Low power wide area networks, internet of things, wireless communications, unslotted aloha, LoRa, stochastic geometry, interference analysis.**

I. Introduction

THE Internet of Things (IoT) is widely adopted in such areas as home automation, u-Health and environment. In IoT, it is essential that things can communicate with their surroundings widely and collect or transmit information with low power consumption, for which Low Power Wide Area (LPWA) network technologies are proposed. However, LPWA technologies achieve the objectives through the trade-off with low data rate (typically in orders of tens of kilobits per seconds) and higher latency (typically in orders of seconds or minutes). Up to date, three technologies are proposed for those use cases of low-power, delay tolerant and low rate transmissions, Narrow Band (NB)-IoT, LoRa and SigFox. These technologies have many different features, and especially differ in that NB-IoT adopts licensed band with existing infrastructure, while as LoRa and SigFox adopt unlicensed band requiring new infrastructure for service.

Lots of work have been carried on for the effect on the coverage by analyzing the interference. Signal activity and power levels for LoRa and SigFox were measured for Industrial, Scientific, and Medical band (863-870 MHz) in the city of Aalborg, Denmark [2]. The coverage and capacity of SigFox and LoRaWAN in urban environments were analyzed [3].

Manuscript received November 28, 2017; revised January 11, 2018; accepted January 13, 2018. Date of publication January 24, 2018; date of current version April 7, 2018. This work was supported by Institute for Information & communications Technology Promotion (IITP) grant funded by the Korea government (MSIP) (No.2016-0-00209). The associate editor coordinating the review of this paper and approving it for publication was F. Wang. *(Corresponding author: Youngnam Han.)*

The authors are with the Department of Electrical Engineering, Korea Advanced Institute of Science and Technology, Daejeon 305-701, South Korea (e-mail: jtyim@kaist.ac.kr; ynhan@kaist.ac.kr).

Digital Object Identifier 10.1109/LCOMM.2018.2797274

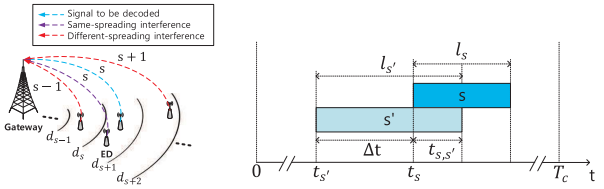

(a) LoRaWAN model (b) Packet collision model

Fig. 1. System model.

Moreover, the coverage of GPRS, NB-IoT, LoRa, and SigFox was compared in a realistic scenario by simulation [4]. Especially for LoRa, a mathematical analysis on its coverage was conducted in [5] via stochastic geometry [6]. However, a little work has been done to maximize the massive connectivity (MC) which is another important feature for LPWA IoT.

In LoRa, a Chirp Spread Spectrum (CSS) modulation technique [1] is adopted to accommodate multiple users in a single channel. It is known that the CSS modulation achieves low receiver sensitivities making long range communications possible. Also, it is known that CSS interference comes mostly from the same-spreading factor (SF) signals, and has a pseudo-orthogonal characteristic with different-SF signals [1]. In order to analyze the MC, we consider low receiver sensitivities and interferences of CSS modulation.

We investigated the MC in LoRa and proposed a sub-optimal SF allocation method by considering the effects of same/different-SF interference under unslotted ALOHA protocol. First, we derived the average system PSP by stochastic geometry. Then, realizing that MC can be achieved by maximizing average system PSP, we formulate an optimization problem and proposed an SF allocation scheme.

II. System Model

We consider an uplink LoRa system as shown in Fig. 1a where N EDs are distributed in a single cell. EDs are located from a homogeneous Poisson point process (PPP) Φ on the Euclidean plane $\mathbb{R}^2$ with intensity $\lambda = \frac{\bar{N}}{\pi R_C^2}$, where R_C is the cell radius and $\bar{N}$ is the mean of Poisson random variable N. Each ED selects an SF s and transmits a packet, where s ($\in \mathbb{S} = \{1, 2, \ldots, 6\}$ and $S = |\mathbb{S}|$) is the index assigned for corresponding SF in Tab I. And these EDs compete with each other through unslotted ALOHA random access protocol within a given contention time T_c.

A. Collision Overlap Time ($t_{s,s'}$) in Unslotted ALOHA

For interference by collisions, we define the collision overlap time $t_{s,s'}$ (Fig. 1b) between packets of SF s and s' and derive its probability density function (PDF). l_s is the length of packet with SF s, $s \in \mathbb{S}$. Because LoRa assumes unslotted ALOHA protocol, $t_{s,s'}$ does not depend on which EDs are transmitting, but on its packet durations. Also, in unslotted

ALOHA, each ED with SF s randomly chooses its transmission start time t_s, where $t_s \sim U(0, T_c' = (T_c - l_s))$ for contention window, T_c. Here, we can assume that $T_c' \cong T_c$ because T_c is sufficiently longer than l_s. By defining Δt as the time difference between the transmission start times of two colliding packets of SF s and s' (i.e., $\Delta t = t_s - t_{s'}$), the PDF of Δt can be derived as $f_{\Delta t}(t) = \max\left(\frac{1}{T_c}\left(1 - \left|\frac{t}{T_c}\right|\right), 0\right)$. From $f_{\Delta t}(t)$, we can get the pdf of $t_{s,s'}$(see Fig. 1b, where $l_s < l_{s'}$ and $t_{s'} < t_s < t_{s'} + l_{s'}$). Assuming that l_s is shorter than $l_{s'}$ (Since, for $l_s > l_{s'}$, it can be seen as symmetric case with l_s and $l_{s'}$ interchanged, we provide analysis for this case), we can derive the distribution of $t_{s,s'}$ from $f_{\Delta t}(t)$ as follows

$$f_{t_{s,s'}}(t) = \frac{1}{T_c}\left(T_c - l_{s'} - l_s + \frac{l_s^2 + l_{s'}^2}{2T_c}\right)\delta(t) + \frac{1}{T_c}\left(l_{s'} - l_s - \frac{(l_{s'} - l_s)^2}{2T_c}\right)\delta(t - l_s) + \frac{2}{T_c^2}t + \frac{1}{T_c}\left(2 - \frac{l_s + l_{s'}}{T_c}\right), \quad (1)$$

where $\delta(\cdot)$ is the Dirac-delta function. In (1), the first term on the righthand side is for the event when there is no collision and the second term comes from the observation that the packet with smaller SF s' is included in the packet of larger SF s packet. The last two terms are for the case when the packets overlap each other in t.

B. SIR Model

The reference packet to be decoded has multiple signal-to-interference ratios (SIR) from $\mathbb{I}_{s'}$ for each s' ($\mathbb{I}_{s'}$, a set of interfering EDs of SF s', $s' \in \mathbb{S}$). Then, we define the SIR of packet with SF s interfering with $\mathbb{I}_{s'}$ as

$$\gamma_{s,s'} = \frac{PgA_0r^{-\alpha}}{\sum_{k\in\mathbb{I}_{s'}} P\frac{t_{s,s'}}{l_{s'}}g_kA_0r_k^{-\alpha}} = \frac{PA_0gr^{-\alpha}}{I_{s,s'}}, \quad (2)$$

where P is the transmit power of each ED, g (or g_k) is the Rayleigh fading channel between gateway (GW) and ED located at r (or interfering ED k), $A_0 = c/4\pi f$ which comes from the Friis transmission equation with the carrier frequency f, c is the light velocity and α is the path loss exponent. And, r (r_k) is the distance between the GW and ED (interfering ED k). The packets are not synchronized under unslotted ALOHA, so we need to normalize interfering power value in (2) by $\frac{t_{s,s'}}{l_{s'}}$. The reason behind this is that if the channel coding make use of an interleaver, the interfering energy between colliding packets can be spread out.

C. SF Allocation in LoRa [5]

In order for the packet with SF s to be successfully decoded in a GW, its received power must exceed a receiver sensitivity q_s (condition I) and its SIR contaminated by the interference with packets of SF s' ($s' \in \mathbb{S}$), $\gamma_{s,s'}$, must also exceed the relative threshold $T_{s,s'}$ (condition II) for all s', simultaneously ($T_{s,s'}$ is given by the element of $\mathbf{T}$ in [1] which is the threshold matrix of LoRa).

In LoRa, the chirp symbol duration can be expressed as $T_s = 2^{SF}/BW$ [1], where SF is a spreading factor and BW is bandwidth. T_s doubles for every increase in SF. As a result, a packet length l_s, which is multiples of T_s, has a different value for each SF s. Actually, an increase in packet duration for a chirp gives the message higher robustness to noise, resulting in a low required signal-to-noise ratio threshold. For each SF s, receiver sensitivity $q_s = -174 + 10\log_{10}B + NF + SNR_s$ where the constant (-174 dBm) is the thermal noise density, and NF is the noise figure margin at GW (6 dB). A typical example for system parameters is provided in Tab. I when $B = 125$ KHz and 25 byte message [5].

TABLE I
CSS MODULATION PROPERTIES OF A 25 BYTE MESSAGE [5]

SF	s	Data Rate kbps	Packet Duration l_s sec	Receiver Sensitivity q_s dBm	SNR_s dB	Range m
7	1	5.47	0.036	-123	-6	$[d_1, d_2]$
8	2	3.13	0.064	-126	-9	$[d_2, d_3]$
9	3	1.76	0.113	-129	-12	$[d_3, d_4]$
10	4	0.98	0.204	-132	-15	$[d_4, d_5]$
11	5	0.54	0.365	-134.5	-17.5	$[d_5, d_6]$
12	6	0.29	0.682	-137	-20	$[d_6, d_7]$

From q_s, we can deduce that the SF to satisfy q_s gets smaller as the ED gets closer to the GW. In other words, the farther the ED is from the GW, the higher SF the ED should be allocated to. It means that there are boundaries which is determined from the receiver sensitivity (condition I). This results in the predefined SF allocation intervals $[d_s, d_{s+1}]$ shown in Fig. 1a. However, the amount of interference is also related to these intervals, the intervals should be determined adaptively considering condition II. To be specific, the increase in the number of long messages could cause higher probability of collision between packets due to the increase in the longer interval of high SF messages, causing severe same/different-SF interferences. So, for EDs, it is important to assign a proper $[d_s, d_{s+1}]$ to meet both conditions.

III. PROBLEM FORMULATION

The MC can be defined as the average number of EDs which meet both conditions $PA_0gr^{-\alpha} \geq q_s$ and $\gamma_{s,s'} \geq T_{s,s'}$ for all s'. Then, MC can be mathematically written as (3) where $\mathcal{I}_A(x)$ is an indicator function, $f_{g,I_{s,s'}}(x,i)$ is the joint PDF of random variables g and $I_{s,s'}$, $f_R(r) = \frac{2r}{R_C^2}$ and $\mathbb{P}[SF = s|r]$ is the probability that ED located at r will send a packet with SF s. $\bigcap$ is the 'intersection' of sets. (a) holds since $\int_X \mathcal{I}_A(x)d\mathbb{P} = \int_X d\mathbb{P} = \mathbb{P}(A)$. And, (b) holds because of the fact that the choice of SF is determined from the predefined interval $[d_s, d_{s+1}]$. Therefore, $\mathbb{P}[SF = s|r]$ is 1 in $[d_s, d_{s+1}]$, and 0 otherwise.

Then, the average system PSP over all EDs, $\overline{PSP}$, can be obtained as $\sum_{s\in\mathbb{S}}\int_{d_s}^{d_{s+1}} PSP_s(r)f_R(r)dr$. Since $\bar{N}$ is a constant, we can conclude that maximizing $\overline{PSP}$ is equivalent to maximizing MC.

A. Average System PSP

$$\overline{PSP} = \sum_{s\in\mathbb{S}}\int_{d_s}^{d_{s+1}} PSP_s(r)f_R(r)dr. \quad (4)$$

$$
\begin{aligned}
&\{\text{Average \# of EDs satisfying both conditions}\}\\
&= \int_0^{2\pi}\int_0^{R_C}\int_0^{\infty}\int_0^{\infty}\sum_{s\in\mathbb{S}}\mathbb{P}[SF=s|r]\mathcal{I}_{\left\{\bigcap_{s'\in\mathbb{S}}\left\{\frac{PA_0gr^{-\alpha}}{I_{s,s'}}\geq T_{s,s'}\right\}\right\}\bigcap\{PA_0gr^{-\alpha}\geq q_s\}}(x,i)\times\lambda\times r\times f_{g,I_{s,s'}}(x,i)\,dx\,di\,dr\,d\theta\\
&\overset{(a)}{=} \bar{N}\int_0^{R_C}\sum_{s\in\mathbb{S}}\mathbb{P}[SF=s|r]\mathbb{P}\left[\left\{\bigcap_{s'\in\mathbb{S}}\{\gamma_{s,s'}\geq T_{s,s'}\}\right\}\bigcap\{PA_0gr^{-\alpha}\geq q_s\}\middle| r\right]\times\frac{2r}{R_C^2}\,dr\\
&= \bar{N}\int_0^{R_C}\sum_{s\in\mathbb{S}}\mathbb{P}[SF=s|r]PSP_s(r)f_R(r)\,dr \overset{(b)}{=} \bar{N}\sum_{s\in\mathbb{S}}\int_{d_s}^{d_{s+1}}PSP_s(r)f_R(r)\,dr
\end{aligned}
\tag{3}
$$

And, $PSP_s(r)$ can be expressed as follows

$$
\begin{aligned}
&PSP_s(r)\\
&= \mathbb{P}\left[\left\{\bigcap_{s'\in\mathbb{S}}\{\gamma_{s,s'}\geq T_{s,s'}\}\right\}\bigcap\{PA_0gr^{-\alpha}\geq q_s\}\middle| r\right]\\
&\overset{(a)}{\geq} \mathbb{P}\left[\bigcap_{s'\in\mathbb{S}}\{\gamma_{s,s'}\geq T_{s,s'}\}\middle| r\right]\mathbb{P}\left[PA_0gr^{-\alpha}\geq q_s|r\right]\\
&\overset{(b)}{\geq} \left[\prod_{s'\in\mathbb{S}}\mathbb{P}[\gamma_{s,s'}\geq T_{s,s'}|r]\right]\mathbb{P}[PA_0gr^{-\alpha}\geq q_s|r].
\end{aligned}
\tag{5}
$$

Inequality (a) is due to the fact that the conditioned probability is greater than the unconditioned probability because the given condition limits the minimum value of the numerator in $\gamma_{s,s'}$ for all s'. Inequality (b) holds due to Fortuin, Kastelynm, Ginibre (FKG) inequality [8]. For that, we need the followings.

For the PPP, let $\omega = (a_1, a_2, \ldots, a_n, \ldots)$ for $n \in \mathbb{N}$, and $a_n = 1$ if ED_n is active and $a_n = 0$ otherwise. Then $\omega' \succeq \omega$ if $a'_n \geq a_n$, $\forall n$. From (2), $\gamma_{s,s'}$ decreases as the number of interfering EDs increases, i.e., $\gamma_{s,s'}(\omega) \leq \gamma_{s,s'}(\omega')$ if $\omega' \succeq \omega$. Thus, the event $\{\gamma_{s,s'} \geq T_{s,s'}\}$ for each SF s' is a decreasing event [7], since if $\omega' \in \{\gamma_{s,s'} \geq T_{s,s'}\}$ and $\omega' \succeq \omega$, then $\omega \in \{\gamma_{s,s'} \geq T_{s,s'}\}$. In other words, these events are positively correlated. Hence, by applying FKG inequality for these events, we can get the lower bound of condition II.

For the last line of (5), we should derive the SIR Complementary Cumulative Distribution Function (CCDF) for each s', which can be written as

$$
\begin{aligned}
&\mathbb{P}[\gamma_{s,s'}\geq T_{s,s'}|r]\\
&\qquad = \mathbb{P}\left[g\geq\frac{T_{s,s'}I_{s,s'}}{PA_0r^{-\alpha}}\middle| r\right]\overset{(a)}{=}\mathbb{E}_{I_{s,s'}}\left[e^{-\frac{T_{s,s'}r^{\alpha}I_{s,s'}}{PA_0}}\right].
\end{aligned}
\tag{6}
$$

(a) follows from the fact that $g \sim \exp(1)$. Then, the Laplace transform of the interference $I_{s,s'}$, $\mathcal{L}_{I_{s,s'}}(z)$ can be written as

$$
\begin{aligned}
\mathcal{L}_{I_{s,s'}}(z) &\overset{(a)}{=} \mathbb{E}_{t_{s,s'},r_k}\left[\prod_{k\in\mathbb{I}_{s'}}\frac{1}{1+zP\frac{t_{s,s'}}{l_{s'}}A_0r_k^{-\alpha}}\right]\\
&\overset{(b)}{=} \mathbb{E}_{r_k}\left[\prod_{k\in\mathbb{I}_{s'}}\mathbb{E}_{t_{s,s'}}\left[\frac{1}{1+zP\frac{t_{s,s'}}{l_{s'}}A_0r_k^{-\alpha}}\right]\right],
\end{aligned}
\tag{7}
$$

where $z = \frac{T_{s,s'}r^{\alpha}}{PA_0}$. (a) comes from the independence among $t_{s,s'}$, g_k and r_k, and $g_k \sim \exp(1)$. (b) comes from the fact that $t_{s,s'}$ for all EDs using SF s' are independent of each other.

By using the probability generating functional of homogeneous PPP [6] to (7), it can be further written as:

$$
\begin{aligned}
\mathcal{L}_{I_{s,s'}}(z) = \exp\Bigg(-2\pi\lambda\int_{d_{s'}}^{d_{s'+1}}\Bigg(1-\mathbb{E}_{t_{s,s'}}&\\
\times\left[\frac{1}{1+zP\frac{t_{s,s'}}{l_{s'}}A_0x^{-\alpha}}\right]\Bigg)xdx\Bigg).&
\end{aligned}
\tag{8}
$$

So, we can obtain the closed form for $\mathbb{E}_{t_{s,s'}}[\cdot]$ applying the PDF (1) of $t_{s,s'}$, which results in (9). With (9), the integral of (8) has the general solution which can be solved by using an analytical solver, such as *Mathematica*. Then, by substituting (8) into (6), and then into (5) with $\mathbb{P}[PA_0gr^{-\alpha} \geq q_s|r] = \exp(-q_sr^{\alpha}/PA_0)$, the lower bound of (4) can be obtained. However, it is not possible to get the closed-form for (4), so the Riemann summation can be adopted for numerical calculation.

B. Optimization Problem and Solution

In this subsection, we propose an algorithm to determine $[d_s, d_{s+1}]$ maximizing (4). We start from (5) because the difference between (4) and a lower bound (5) is small, which will be verified. In order to make (5) tractable, we made the following assumptions. The different-SF interference is ignored. Moreover, only the probability event when $t_{s,s'} = 0$, which is the largest portion due to large T_c, is considered in (1). We use the approximation, $\exp(-x) \simeq (1-x)$ for small x. With approximations, we can formulate the optimization problem, $\max_{d_2,\ldots,d_S}\overline{PSP}$ as:

$$
\begin{aligned}
\max_{d_2,\ldots,d_S}\sum_{s=1}^{S}&\left[\frac{(d_{s+1}^2-d_s^2)}{R_C^2}-\frac{2q_s(d_{s+1}^{\alpha+2}-d_s^{\alpha+2})}{(\alpha+2)PA_0R_C^2}\right]\\
&\times\left[1-\lambda\pi\left(d_{s+1}^2-d_s^2\right)\left(\frac{2l_s}{T_c}-\frac{l_s^2}{T_c^2}\right)\right]
\end{aligned}
\tag{10}
$$

subject to $d_s \leq d_{s+1}, \forall s \in \mathbb{S}$, where $d_1 = \delta$ and $d_{S+1} = R_C$ are fixed values (δ is set to avoid the singular point in path loss model). The first bracket within the summation of (10) is for condition I. In the second bracket (i.e., condition II probability), we can deduce that one interfering ED reduces the probability of condition II by almost $\frac{2l_s}{T_c}$ on the average. We conjecture that $\frac{2l_s}{T_c}$ comes from the uniform random choice of slots in unslotted ALOHA protocol. Therefore, maximizing $\overline{PSP}$ corresponds to determining SF regions and so allocating SFs to each ED.

If α is not an integer, (10) becomes a nonlinear programming (NLP) problem with the bounded variation. Although the

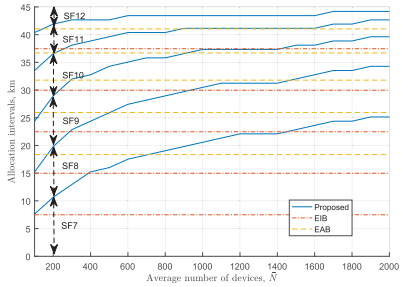

Fig. 2. Average number of EDs v.s. Allocation intervals.

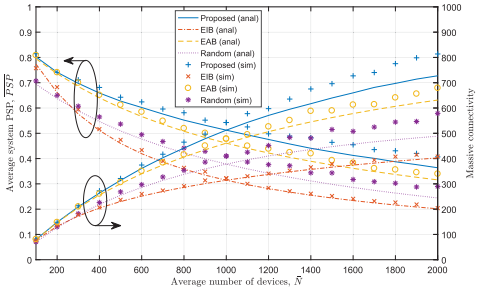

Fig. 3. Average number of EDs v.s. (Average system PSP, MC).

complexity is high with multiple variables, this problem can be solved with a global optimization solver, such as multilevel coordinate search (MCS) in *MATLAB* or MathOptimizer and Global optimization packages of *Mathematica*.

And, the proposed method can be implemented as follows. ED periodically sends its location and uplink channel information to a GW, with a long interval. Then the GW allocates SF to each ED by the proposed SF allocation, which will be updated with the next channel report. It might have a limitation because EDs periodically send information to the GW, which requires more power and complexity, but negligible compared to other schemes. And the proposed scheme is also beneficial to for long-term changes in the channel.

IV. Results and Discussions

We make simulations for performance comparison, where path loss exponent is assumed to be 2.7 (suburban scenario), f is assumed to be 867 MHz (for LoRa in Europe), the average number of EDs varies from 100 to 1000, and EDs are distributed within a single GW coverage of radius $R_C = 45$ km. P was 14 dBm and T_c is set to 60 sec. The other parameters are provided as in Tab. I. For the performance comparison, we adopted 3 other existing schemes such as;

- **Equal-Interval-Based (EIB) scheme** [5] which determine $[d_s, d_{s+1}]$, according to $(d_{s+1} - d_s) = R_C/S$,
- **Equal-Area-Based (EAB) scheme** which determine $[d_s, d_{s+1}]$, based on $d_s = R_C\sqrt{(s-1)/S}$ that makes the areas of doughnuts equal.
- **Random scheme** which allocates SFs by uniform random choice, not depending on the location of the ED.

The allocation intervals for proposed, EIB and EAB scheme are shown in Fig. 2. From Fig. 2, it can be said that, as $\overline{N}$ increases, it get more difficult for each ED to satisfy condition II, so the proposed scheme makes the lowest SF region larger to reduce collisions. In other words, when $\overline{N}$ is large, it is more advantageous for maximizing $\overline{PSP}$ to increase the probability for condition II than to increase the probability for condition I.

Monte Carlo simulations and analysis results are presented in Fig. 3 for the validation of the lower bound of (5). The gap between the numerical lower bound in (4) and simulation lies within an acceptable bound, confirming that the overall performance of LoRa can be analyzed through the derived lower bound. Also, this tight bound means that each event considered in (5) is almost independent.

From Fig. 3, we can make the following discussions. First, we can confirm that EIB scheme works worse than Random scheme because condition II becomes difficult to be satisfied when $\overline{N}$ increases. In case of EAB scheme when EDs were equally allocated in each SF region, the influence of interferences can be reduced to some extent, resulting in better performance than Random and EIB schemes. The proposed scheme is superior to all other schemes in terms of MC because both conditions are considered. From simulations with $\bar{N} = 2000$, the proposed method can provide stable 810 EDs satisfying both conditions, which is about 22% increase in MC over EAB. These results are based on the active EDs only, so the total number of EDs served during the contention period will be large by the inverse of activity factor.

References

[1] C. Goursaud and J.-M. Gorce, "Dedicated networks for IoT: PHY/MAC state of the art and challenges," *EAI Endorsed Trans. Internet Things*, vol. 1, no. 1, pp. 1–11, Oct. 2015.
[2] M. Lauridsen, B. Vejlgaard, I. Z. Kovács, H. Nguyen, and P. Mogensen, "Interference measurements in the European 868 MHz ISM band with focus on LoRa and SigFox," in *Proc. IEEE WCNC*, San Francisco, CA, USA, Mar. 2017, pp. 1–6.
[3] B. Vejlgaard, M. Lauridsen, H. Nguyen, I. Z. Kovács, P. Mogensen, and M. Sorensen, "Interference impact on coverage and capacity for low power wide area IoT networks," in *Proc. IEEE WCNC*, San Francisco, CA, USA, Mar. 2017, pp. 1–6.
[4] M. Lauridsen, H. C. Nguyen, B. Vejlgaard, I. Kovacs, P. E. Mogensen, and M. Sørensen, "Coverage comparison of GPRS, NB-IoT, LoRa, and SigFox in a 7800 km^2 area," in *Proc. IEEE VTC Spring*, Sydney, NSW, Australia, Jun. 2017, pp. 1–5.
[5] O. Georgiou and U. Raza, "Low power wide area network analysis: Can LoRa scale?" *IEEE Wireless Commun. Lett.*, vol. 6, no. 2, pp. 162–165, Apr. 2017.
[6] M. Haenggi, *Stochastic Geometry for Wireless Networks*. Cambridge, U.K.: Cambridge Univ. Press, 2013.
[7] R. Vaze, K. T. Truong, S. Weber, and R. W. Heath, Jr., "Two-way transmission capacity of wireless ad-hoc networks," *IEEE Trans. Wireless Commun.*, vol. 10, no. 6, pp. 1966–1975, Jun. 2011.
[8] G. R. Grimmett, *Percolation*. New York, NY, USA: Springer-Verlag, 1989.

$$E_{t_{s,s'}}\left[\frac{1}{1+zP\frac{t_{s,s'}}{l_{s'}}A_0x^{-\alpha}}\right] = \frac{1}{T_c}\left(T_c - l_{s'} - l_s + \frac{l_{s'}^2 + l_s^2}{2T_c}\right) + \frac{1}{1+zPA_0x^{-\alpha}}\frac{1}{T_c}\left(l_{s'} - l_s - \frac{(l_{s'}-l_s)^2}{2T_c}\right) + \frac{l_{s'}^2\frac{2}{T_c^2}}{zPA_0x^{-\alpha}} + \frac{(zPA_0x^{-\alpha})\frac{l_{s'}}{T_c}\left(2 - \frac{l_s+l_{s'}}{T_c}\right) - \frac{2l_{s'}^2}{T_c^2}}{(zPA_0x^{-\alpha})^2}\log(1+zPA_0x^{-\alpha}) \quad (9)$$